

BETIS: Bidimensional Exploration of the warm-Temperature Ionised gas

González-Díaz, R.^{1,2,3}, Rosales-Ortega, F. F.², and Galbany, L.^{1,3}

¹ Institute of Space Sciences (ICE-CSIC), Campus UAB, Carrer de Can Magrans, s/n, E-08193 Barcelona, Spain.

² Instituto Nacional de Astrofísica, Óptica y Electrónica (INAOE-CONAHCyT), Luis E. Erro 1, 72840 Tonantzintla, Puebla, México.

³ Institut d'Estudis Espacials de Catalunya (IEEC), 08860 Castelldefels, Barcelona, Spain.

Abstract

The extraplanar diffuse ionised gas (eDIG) is a key component for understanding the feedback processes that connect galactic discs and their halos. We present the Bidimensional Exploration of the warm-Temperature Ionised Gas (BETIS) project, the aim of which is to explore the possible ionisation mechanisms and characteristics of the eDIG. We use a sample of eight edge-on galaxies observed with the Multi-Unit Spectroscopic Explorer (MUSE) integral field spectrograph (IFS) and apply the methodology developed in the first paper of the BETIS project for obtaining binned emission line maps. We find that the vertical and radial profiles of the $[\text{N II}]/\text{H}\alpha$, $[\text{S II}]/\text{H}\alpha$, $[\text{O III}]/\text{H}\beta$, and $[\text{O I}]/\text{H}\alpha$ ratios depict a complex ionisation structure within galactic halos —which is influenced by the spatial distribution of H II regions across the galactic plane as observed from our line of sight—, with Lyman continuum photon leakage from OB associations constituting the main ionisation source. We ascertain that shocks induced in the interstellar medium by star formation (SF)-related feedback mechanisms represent a promising secondary ionisation source of the eDIG. We present a suite of models integrating ionisation mechanisms arising from fast shocks and photoionisation associated with star formation. When applied to the classical Baldwin-Phillips-Terlevich (BPT) diagrams, these models reveal that the ionisation budget of the eDIG ranges from 20% to 50% across our sample, with local variations of up to 20% within individual galaxy halos. This correlates with the presence of filaments and other structural components observed within galaxy halos.

1 Introduction

The extraplanar diffuse ionised gas (eDIG), plays a crucial role in the physical processes driving the exchange of gas, metals, and energy between the galactic disc and halo, influencing the evolution of disc galaxies (e.g. [16, 13].)

Several mechanisms has been proposed to explain the ionisation of the eDIG. For instance the hot low-mass evolved stars (HOLMES; e.g. [6]), or turbulent mixing layers (TML, e.g. [3]).

To advance the characterisation and exploration of the ionisation of extraplanar gas, it is crucial to study the impact of the various structures found in the halos of individual galaxies, such as filaments, plumes, and bubbles. Previous studies using IFS presented large samples of low-resolution galaxies —with the exception of those conducted with the MUSE instrument—, but focused on just one galaxy or failed to inquire into the connection between disc and halo that originates these structures and changes the ionisation conditions (e.g. [11, 5]).

We present the second study of the Bidimensional Exploration of the warm-Temperature Ionised gaS (BETIS) project, the aims of which are to characterise the eDIG and to explore its possible ionisation mechanisms by studying a sample of edge-on galaxies.

2 The data

The characterisation of the eDIG and the exploration of its ionisation mechanisms requires spatially resolved data and spectral information. For this reason we use Multi Unit Spectroscopic Explorer (MUSE, [2]), data to undertake this task, that brings 1 arcmin² of field of view (FoV), with a spatial and spectral sampling of 0.2×0.2 arcsec and 1.25 Å respectively within a spectral range of 4650 – 9300 Å. In particular, we use the sample of [4], since this type of investigation requires more constraints compared to the face-on case, since we are navigating within the galactic halo, where the signal-to-noise ratio of the observed emission line (S/N, [7]) is lower. Consequently, besides high resolution, we require data as deep as possible to observe low surface brightness lines such as [O I] and [O III], alongside data of sufficient quality to measure the [O I] line without interference from sky lines, and [4] sample meet these criteria. In addition, the binned emission line maps were obtained following the methodology developed in [7].

3 The link between the galactic plane and the eDIG

The presence of structures in the halo becomes more evident when examining the maps of the [N II]/H α , [S II]/H α , [O I]/H α , and [O III]/H β line ratios. These maps reveal new ionised features that were initially invisible when only examining the H II images. For instance, Fig. 1 shows the binned maps of the mentioned lines ratios of the ESO157-49 galaxy. The images show the intricate and asymmetrical structure of the eDIG. Having differences of 0.4 dex in the [S II]/H α ratio along the major axis and over 0.8 dex in [N II]/H α . Additionally, the line ratios increase with respect to the distance from the midplane, a phenomenon that

is well-documented in the literature [11]. However, the 2D spectroscopic analysis of the eDIG allows to recognise that the variation of the line ratios are dependent not only on height, but along the major axis distance (MAD) of the galaxy, as seen in 1, which shows the distribution of the eDIG characteristic line ratios with respect the distance from the midplane for ESO157-49. Analogously, this corresponds to the line ratio height distribution in a long-slit located at those MADs and perpendicular to the galactic plane. The integrated distribution of the $[\text{N II}]/\text{H}\alpha$, $[\text{S II}]/\text{H}\alpha$ and $[\text{O I}]/\text{H}\alpha$ line ratios tends to increase in height, reaching a minimum inside the galactic plane. However, in addition to this, when restricting the height distributions to specific MADs, the overall behaviour of the distributions remains consistent, but the line ratios exhibit notable differences, suggesting that the physical conditions in the eDIG are influenced by the distribution of the H II regions emission along the galactic plane.

The correlation between the morphological distribution of star-forming regions in the discs of edge-on galaxies and the shapes and morphology of the halos presents the strongest evidence supporting the interpretation that energy sources from SF within the galaxy discs drive the observed disc-halo interactions [14].

4 The ionisation mechanism of the eDIG

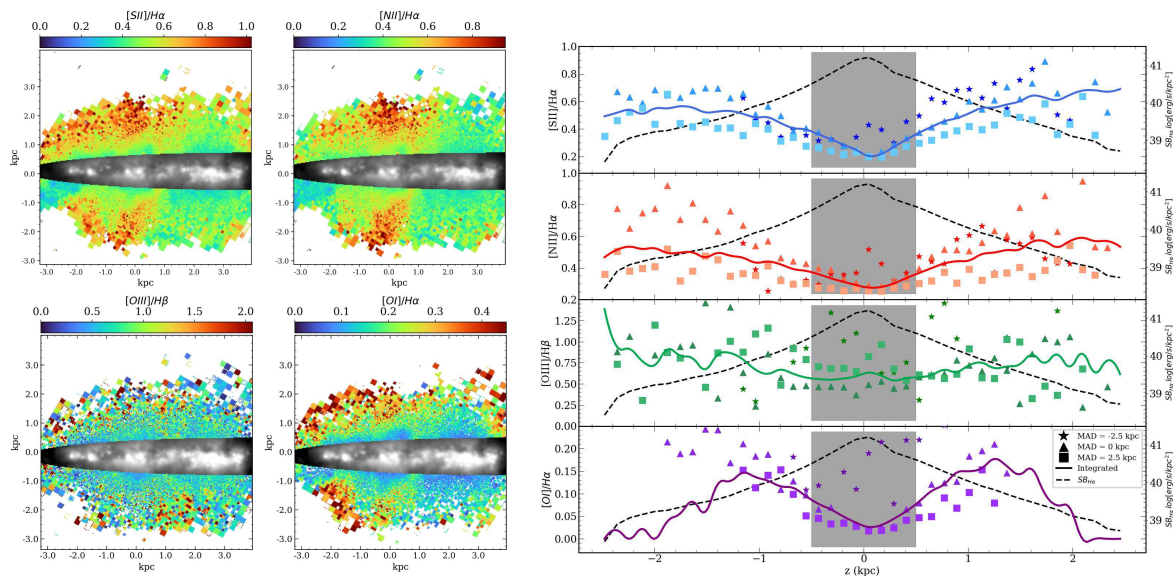


Figure 1: Left: ESO157-49 line ratio maps. We overlay the $\text{H}\alpha$ map of the galactic plane. Right: Distribution of the line ratios with respect the distance from the midplane for the ESO157-49 galaxy. The star-shaped, triangular, and square markers represent the line ratio at that z for MAD = -2.5, 0, and 2.5 kpc, respectively. The solid lines represent the integrated values along the major axis distance. The dashed black line represents the $\Sigma_{\text{H}\alpha}$ height distribution of the galaxy.

In the scenario delineated above, the eDIG emission originates in situ within low-density gas environments, induced by ionising photons propagated from the galactic disc via transparent conduits formed by superbubbles or chimneys. Shocks induced in the ISM by feedback mechanisms, such as supersonic winds originating from high-level SF regions, have been proposed as a significant source of heating for the eDIG. In this scenario, galactic winds are driven by the stellar winds and subsequent SNe of massive stars. These stellar winds create kpc-sized cavities in the ambient ISM on timescales of several million years [12]. Subsequently, these cavities are overrun by SN remnants (SNRs) from the most massive progenitor stars. Both processes occur at velocities exceeding the local sound speed, v_s , in the ISM, thereby generating strong shocks. Fast shocks induce comparable ionised conditions, characterised by an ionisation equilibrium between the hot and cold gas phases and slow mixing within the turbulent layer [15, 5]. We explore the combination of photoionisation from H II regions and ionisation due to fast shocks as simultaneous contributors to the ionisation mechanism of the eDIG. This is achieved by constructing a set of hybrid models that incorporate both star formation and fast shock mechanisms.

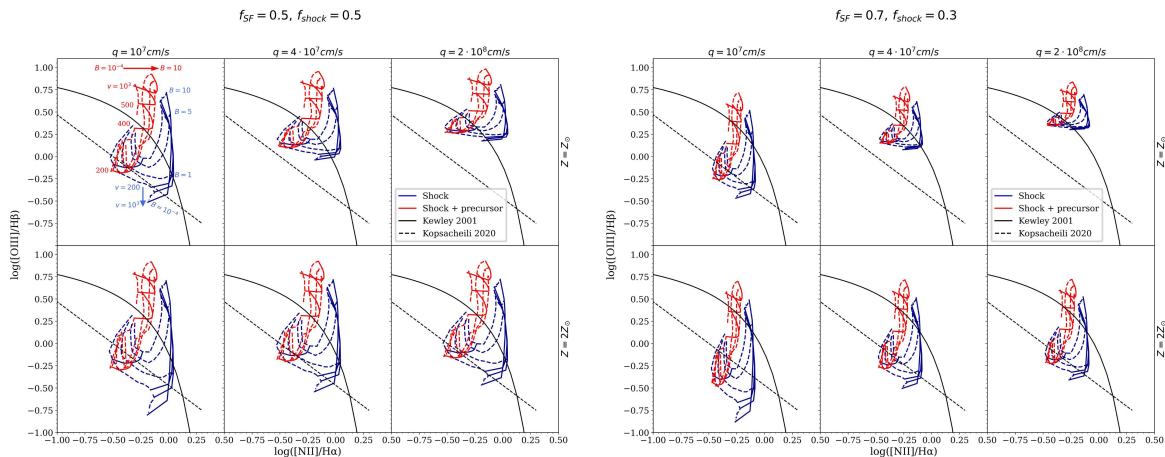


Figure 2: Showcase star formation + fast shocks hybrid models for the [N II] BPT. Left panels correspond to the hybrid models with a contribution of fast shocks of 50% and 50% star formation. Right panels correspond to 30% shocks and 70% star formation. The fast shocks models from [1] correspond to shock velocities of 200 to 1000 km/s and magnetic fields of 10^{-4} to $10 \mu\text{G}\cdot\text{cm}^{3/2}$, assuming shocks + a precursor (red curves) and only shocks (blue lines). The red arrow indicates the direction of increasing magnetic field in the shocks + precursor models, and the blue arrow indicates the direction of increasing shock velocity in the shock-only models.

We firstly consider the photoionisation models for low-metallicity star-forming galaxies of [10]. The grids of this models predict the line ratios involved in the typical BPT diagram for a pure photoionisation regime due to the star formation with ionisation parameters (q) ranging from 10^7 to $2\cdot 10^8$ cm/s and metallicities (Z) from 0.001 to 0.04. Each model grid is computed for electron densities n_e of 10, 10^2 , 10^3 and 10^4 cm^{-3} , assuming either continuous star formation or an instantaneous burst of star formation at 0 Myr.

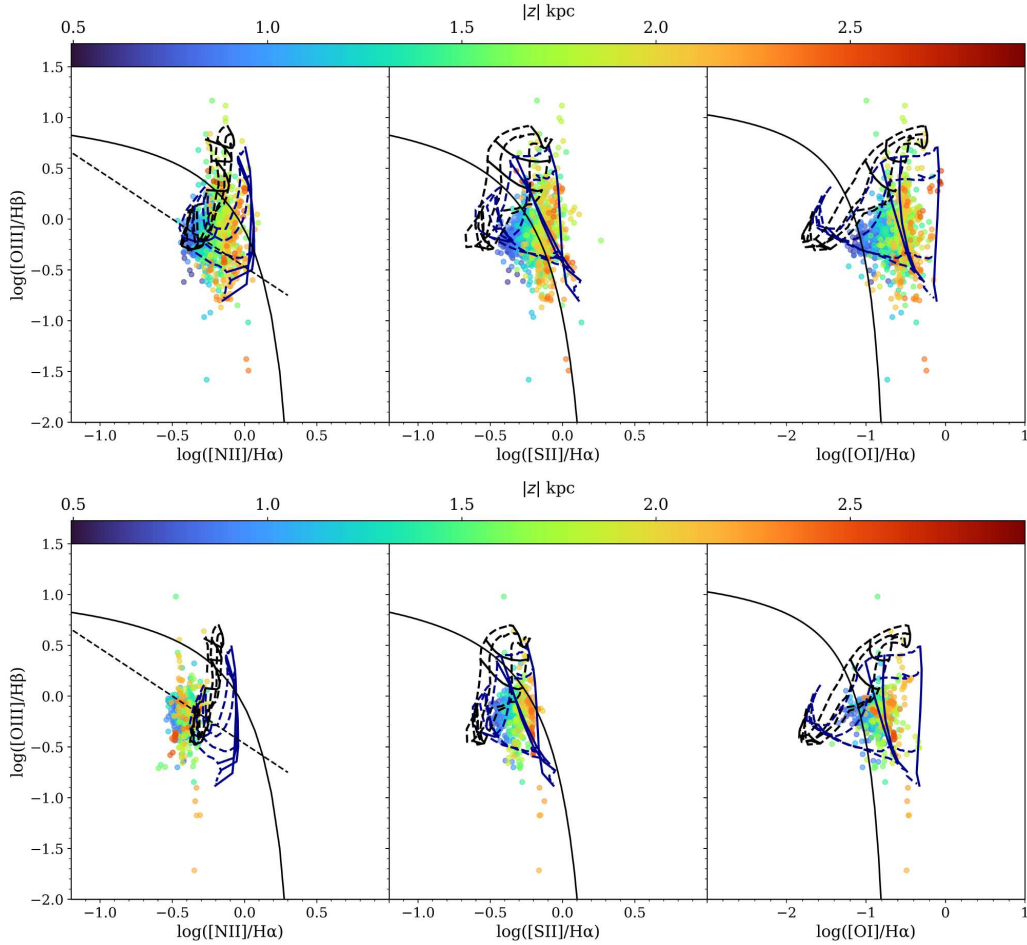


Figure 3: ESO157-49 BPT with hybrid models. Up: BPT for bins between $-0.5 \text{ kpc} < \text{MAD} < 0.5 \text{ kpc}$. Hybrid models correspond to 50% fast shocks and 50% star formation with $Z = 2Z_{\odot}$ and $q = 10^7 \text{ cm/s}$. Down: BPT for bins between $2.25 \text{ kpc} < \text{MAD} < 2.75 \text{ kpc}$. Hybrid models correspond to 30% fast shocks and 70% star formation with $Z = 2Z_{\odot}$ and $q = 10^7 \text{ cm/s}$.

On the other hand, we consider the fast shocks models of [1]. This models predict the flux of the ionising radiation produced by a shock. The flux is dependent on the shock velocity ($f \propto v_s^3$). Therefore, if the shock velocity surpasses the velocity of the photoionisation front (in the case of a low ionisation parameter), the ionising photons are absorbed by the surrounding gas, altering its ionisation state. In another scenario, if $v_s \approx 170 \text{ km/s}$, the ionisation front velocity now exceed the velocity of the shock, pre-ionising the surrounding gas and changing the optical emission lines observed. The fast shocks models of [1] consider this two scenarios, with preshock densities ranging from 0.01 to 1000 cm^{-3} , shock velocities from 100 to 1000 km/s and magnetic field ($B/n^{1/2}$) from 10^{-4} to $100 \mu\text{G}\cdot\text{cm}^{3/2}$ (see [8] for more details).

Figure 2 shows an example of hybrid models for the $[\text{N II}]/\text{H}\alpha$ BPT, with $Z = Z_{\odot}$ and $2Z_{\odot}$, $q = 10^7$, $4 \cdot 10^7$ and $2 \cdot 10^8$ cm/s, and $f_{shock} = 0.5$ and 0.3 . It shows that decreasing f_{shock} shifts the models towards the OB-stars regime, indicating that photoionisation by star formation becomes more significant in the hybrid models. Additionally, increasing the ionisation parameter in the models tends to flatten them vertically, resulting in higher predicted values for the high excitation $[\text{O III}]/\text{H}\beta$ ratio. Besides, increasing the metallicity tends to expand the models, predicting a wider range of both $[\text{O III}]/\text{H}\beta$ and $[\text{N II}]/\text{H}\alpha$ ratios.

For instance, the contribution of fast shocks in the ionisation of the eDIG for ESO157-49 between $-0.5 \text{ kpc} < \text{MAD} < 0.5 \text{ kpc}$ is 50% (Fig. 3); however, this drops to 30% between $2.25 \text{ kpc} < \text{MAD} < 2.75 \text{ kpc}$, where the $\Sigma_{\text{H}\alpha}$ is higher. In this latter case, is clear that bins further from the plane tend to be closer to the fast shock regime in the BPT, being the contribution of the fast shocks dependent with the distribution of H II regions in the galactic plane (see [8]).

Acknowledgments

R.G.D. acknowledges the CONAHCyT scholarship No. 1088965 and INAOE for the PhD program. The authors also acknowledges Manuel Zamora and Raúl Naranjo for allowing us the usage of the Mextli cluster at INAOE. R.G.D and L.G. acknowledge financial support from AGAUR, CSIC, MCIN and AEI 10.13039/501100011033 under projects PID2023-151307NB-I00, PIE 20215AT016, CEX2020-001058-M, and 2021-SGR-01270.

References

- [1] Allen M. G., Groves B. A., Dopita M. A., Sutherland R. S., Kewley L. J., 2008, ApJS, 178, 20
- [2] Bacon R., et al., 2010, SPIE Conference Series Vol. 7735, doi:10.1117/12.856027
- [3] Begelman M. C., Fabian A. C., 1990, MNRAS, 244, 26P
- [4] Comerón S., Salo H., Knapen J. H., Peletier R. F., 2019, A&A, 623, A89
- [5] Dirks L., Dettmar R. J., Bomans D. J., Kamphuis P., Schilling U., 2023, A&A, 678, A84
- [6] Flores-Fajardo N., Morisset C., Stasínska G., Binette L., 2011, MNRAS, 415, 2182
- [7] González-Díaz R., et al., 2024, A&A, 687, A20
- [8] González-Díaz R., Rosales-Ortega, F. F., Galbany, L., 2024, arXiv e-prints, p. arXiv:2406.17123
- [9] Hummel E., Beck R., Dahlem M., 1991, A&A, 248, 23
- [10] Levesque E. M., Kewley L. J., Larson K. L., 2010, AJ, 139, 712
- [11] Levy R. C., et al., 2019, ApJ, 882, 84
- [12] Mayya Y. D., et al., 2023, MNRAS, 521, 5492
- [13] Miller S. T., Veilleux S., 2003, ApJS, 148, 383
- [14] Norman C. A., Ikeuchi S., 1989, ApJ, 345, 372
- [15] Slavin J. D., Shull J. M., Begelman M. C., 1993, ApJ, 407, 83
- [16] Tenorio-Tagle G., Bodenheimer P., 1988, ARA&A, 26, 145